

# An Electrically Modulatable Silicon Waveguide Grating Using an Implantation Technology

Qing Fang, Lianxi Jia, JunFeng Song, Xiaoguang Tu, Mingbin Yu, Andy Eu-jin Lim, Guo Qiang Lo

**Abstract**—The first pn-type carrier-induced silicon Bragg-grating filter is demonstrated. The extinction-ratio modulations are 11.5 dB and 10 dB with reverse and forward biases, respectively. 8-Gbps data rate is achieved with a reverse bias.

**Keywords**—Silicon photonics, Waveguide grating, Carrier-induced, Extinction-ratio modulation.

## I. INTRODUCTION

**B**RAGG-GRATING-BASED optical devices have been using widely in optical communication systems, especial the fiber Bragg grating filter [1], [2]. Due to the low index difference in the optical fiber, the Bragg grating length is normally long. On the other hand, the linear electro-optic coefficient of optical fiber is very low and it is impossible to form PN or PIN junction in optical fiber. So, it is hard to realize high-speed modulation in the fiber Bragg grating filter. Silicon photonics had become an amazing research hotspot in the last decade because of excellent performances and low cost of silicon materials. Many kinds of Silicon Bragg gratings formed by etching process were reported, recently [3]-[5]. Because of the high index difference and plasma dispersion effect in silicon, the size of silicon Bragg grating is small and the modulation speed can be very high. However, this kind of silicon Bragg grating structure is permanent and its reflected wavelength exists in the spectrum once it is formed by etching process. A novel silicon Bragg grating can be formed by ion implantation and the grating finger length can be modulated by a bias. So, the extinction ratio of the reflected wavelength can be modulated with a bias. We demonstrated a PIN-type silicon Bragg grating using ion implantation technology last year [6]. This carrier-induced PIN-type silicon Bragg grating can be modulated under a forward bias and its extinction ratio decreases with the increase of forward bias. However, it is hard to modulate the extinction ratio under a reverse bias because the finger length is hard to change with a reverse bias. In this paper, we demonstrated the first PN-type carrier-induced silicon Bragg grating using the same ion implantation technology on

Qing Fang, Lianxi Jia, Jun Feng Song, Chao Li, Xianshu Luo, Mingbin Yu, and Guo Qiang Lo are with Institute of Microelectronics, A\*STAR (Agency of Science and Technology Research), Singapore (e-mail: fangq@ime.a-star.edu.sg).

Qing Fang is also with Department of Physics, Faculty of Science, Kunming University of Science and Technology, Yunnan, China (e-mail: qingfang.imesemi@yahoo.com.sg) and with Optoelectronic System Laboratory, Institute of Semiconductors, CAS, Beijing, China (e-mail: qingfang@red.semi.ac.cn)

Junfeng Song is also with State Key Laboratory on Integrated opto-electronics, College of Electronic Science and Engineering, Jilin University, Changchun, China (e-mail: songjff@ime.a-star.edu.sg)

SOI platform. The extinction ratio of this PN-type silicon Bragg grating can be modulated under both reverse biases and forward biases. The optical 3dB-bandwidth of 0.45 nm and the ER of 19 dB are achieved on the PN-type Bragg grating. With the carrier injection, the ER modulation is more than 10 dB. With the carrier depletion, the ER modulation is more than 11.5 dB. The electrical modulation speed is fast. An eye-diagram with a data rate of 8 Gbps is measured.

## II. DESIGN AND FABRICATION

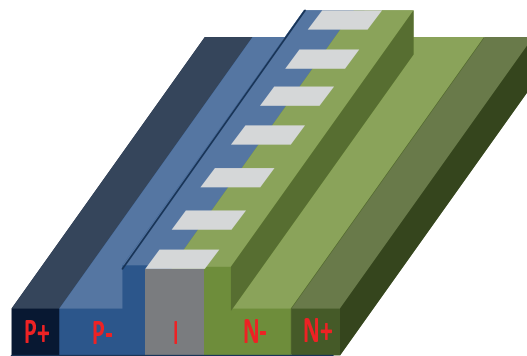


Fig. 1 Schematic of the PN-type carrier-induced Bragg grating. The Bragg grating is composed of the implantation patterns.

The Bragg grating finger is composed of low P and low N implantation, shown in Fig. 1. The PN junction is located at the center of each finger. The intrinsic Si range is designed between each finger of Bragg grating. According to the plasma dispersion effect in silicon, the refractive index of silicon will change with the increase of the ion concentration. The refractive index in P and N implantation area decreases when P and N implantation is processed. On the other hand, the refractive index in the intrinsic Si range is not changed. So, the Bragg grating is formed by ion implantation. In this device, the rib width of silicon waveguide is 400 nm and the height of the rib waveguide is 220 nm. The slab height is 130 nm and the grating length is 2000  $\mu\text{m}$ . The grating period of 310 nm is design for the operation in 1550nm communication window, based on the Bragg equation. The duty cycle of 50:50 is adopted. We use a 248 nm lithography system and fully opening the kind of small structure is a challenge for this lithography tool. So, the pattern compensation design is adopted in the layout to guarantee the PN-type carrier-induced Bragg grating formation. The extinction ratio is dependent on the length of Bragg grating finger which is dominated by the depletion width. For a PN-type junction, the depletion width ( $W$ ) is shown in the below.

$$W = \left[ \frac{2\epsilon(V_{bi} - V)}{e} \left( \frac{N_a + N_d}{N_a N_d} \right) \right]^{1/2} \quad (1)$$

where  $V_{bi}$  is the built-in voltage of the junction,  $V$  is the external voltage,  $N_a$  is the carrier concentration of P-type,  $N_d$  is the carrier concentration of N-type. With increase of the reverse bias, the depletion width increases. Correspondingly, the finger of the carrier-induced Bragg grating becomes shorter and the extinction ratio becomes lower.

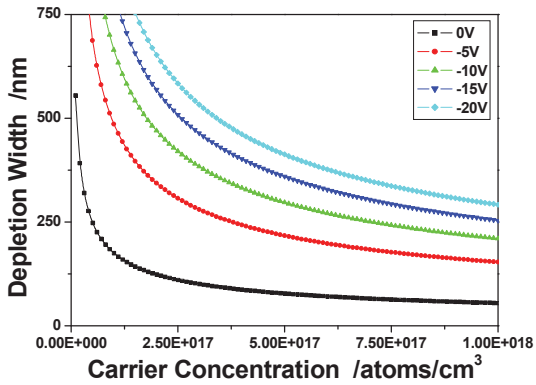


Fig. 2 Depletion width of a PN junction with reverse biases

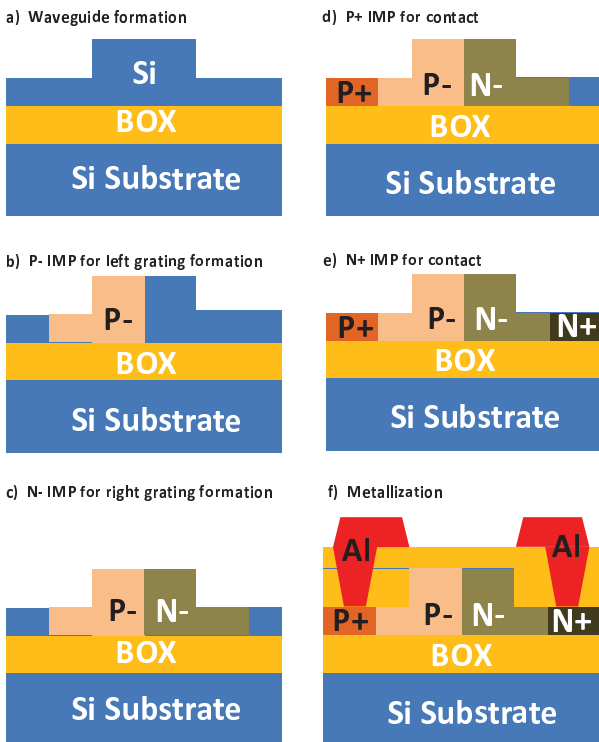


Fig. 3 Process flow of the carrier-induced grating

Fig. 2 shows the relationship between the depletion width and the reverse bias at different carrier concentrations at the PN junction. The design of the carrier concentration is a trade-off in

consideration of the depletion width with/without reverse bias for a good extinction ratio modulation.

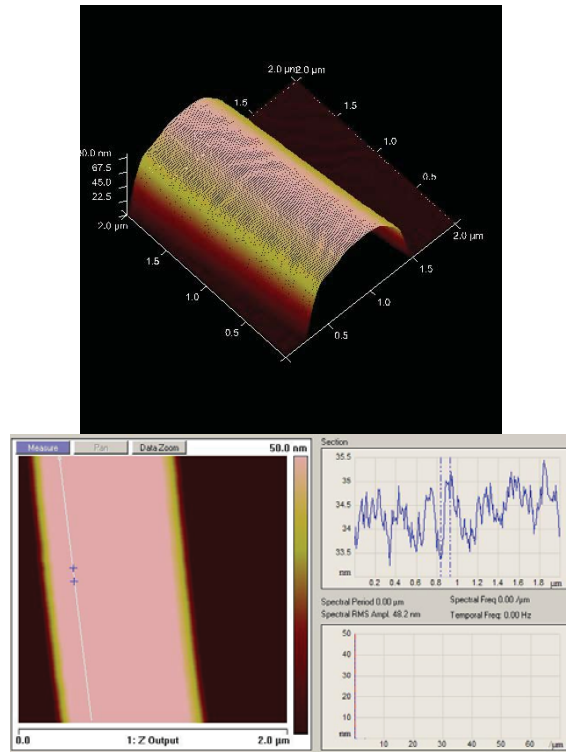


Fig. 4 AFM image and surface roughness of Bragg grating after implantations and annealing

The carrier-induced Bragg grating was fabricated on an 8-inch silicon-on-insulator (SOI) wafer with 220 nm top Si layer and 2 μm buried oxide. The fabrication process is similar to the previously reported PIN-type carrier-induced Bragg grating [6], except the implantation conditions. First, the waveguide pattern was performed using a 248 nm UV lithography and the Si was partially etched to form the slab of 130 nm, shown in Fig. 3 (a). Then, two kinds of low implantations were processed to form the grating pattern in the rib waveguide, shown in Figs. 3 (b), (c). In order to get a uniform implantation in the 220nm-thick silicon waveguide, two kinds of boron ion conditions were processed in Fig. 3 (b). The doses are  $0.5 \times 10^{13}$  ions/cm<sup>2</sup> and  $1.5 \times 10^{13}$  ions/cm<sup>2</sup>. The corresponding energies are 15 KeV and 35 KeV, respectively. The carrier concentration near the junction is around  $7 \times 10^{17}$  atoms/cm<sup>3</sup>. In Fig. 3 (c), the phosphorus ion with the similar doses was implanted under the energies of 30 KeV and 90 KeV, respectively. The carrier concentration near the junction is around  $7 \times 10^{17}$  atoms/cm<sup>3</sup>. After low implantations, the two high implantations were processed to reduce the contact resistivity, shown in Figs. 3 (d), (e). After all implantations and activation, the contact holes were etched by both dry and wet etching methods which were used to avoid Si loss. Finally, 1μm-thick TaN/Al metal stack was deposited and the stack was etched to form the metal line after lithography process. The AFM image of the dosed silicon waveguide is shown in the left

of Fig. 4 after all implantations and annealing. The surface roughness along the dosed silicon waveguide is shown in the right of Fig. 4. The results show that the silicon of less than 1.5 nm is lost in the implantation area. Its contribution to the extinction ratio of reflected wavelength can be negligible.

III. MEASUREMENT RESULTS

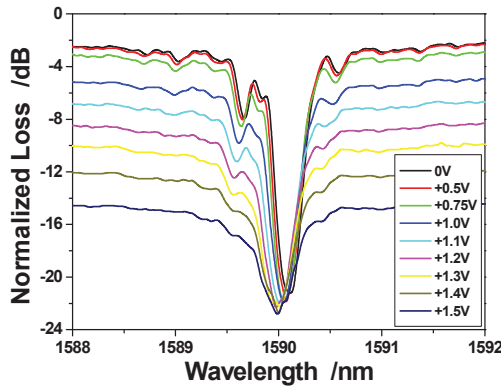


Fig. 5 Optical transmission spectra of PN-type Bragg grating with forward biases

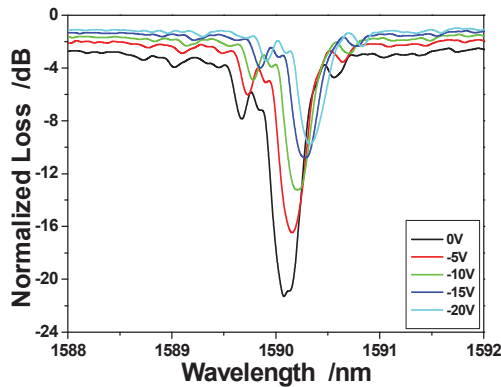


Fig. 6 Optical transmission spectra of PN-type Bragg grating with reverse biases

The measured spectra of this PN-type Bragg grating filter with forwards biases for TE mode is shown in Fig. 5. The transmission loss is 2.5 dB and the reflected wavelength is 1590.15 nm without any bias. The corresponding extinction ratio is ~ 19 dB. In consideration of the propagation loss (2.5 dB/cm) of undoped ridge Si waveguide, the excess optical loss from implantation is ~ 2.0 dB. With increasing the forward bias, the reflected central wavelength is shifted to the short wavelength side. This shift matches the fact that the forward current increases with the applied voltage. According to the carrier plasma dispersion effect, the effective refractive index of the waveguide reduces when the carrier concentration increases. The extinction ratio modulation of more than 10 dB is realized at the forward voltage of 1.5 V. Fig. 6 is the optical transmission spectra with reverse biases. With increasing the reverse bias, the reflected central wavelength is shifted to the long wavelength side. This is different from the shift direction

under the forward bias. Under the reverse bias, the depletion width increases and the carrier concentration decreases near the PN junction. Hence, the effective refractive index of waveguide increases. It causes the reflected wavelength to shift toward the long wavelength side. Moreover, the lower carrier concentration under the reverse bias reduces the optical loss. When the reverse bias is -20 V, the optical loss of this grating reduces to 1.0 dB from 2.5 dB. With increasing of reverse bias, the depletion width at the pn junction increases. Hence, the extinction ratio of grating is modulated. An extinction ratio modulation of more than 11.5 dB is realized in a bias of -20 V. The IV results of the PN-type Bragg grating is shown in Fig. 7. The reverse current is less than 30  $\mu$ A with the reverse bias up to -20 V. So, the thermo-optic effect can be negligible when the bias is 0 ~ -20 V. At the data rate of 8 Gbps, the eye-diagram is measured with a bias of -5 V, shown in Fig. 8.

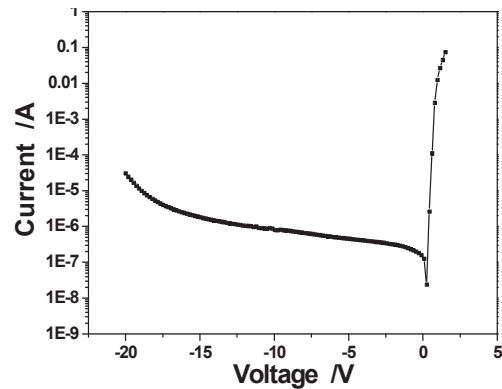


Fig. 7 IV curve of PN-type Bragg grating

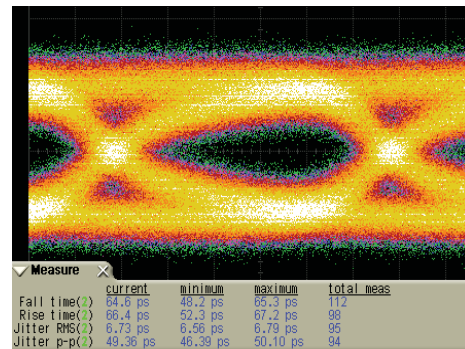


Fig. 8 Measured eye-diagram with 8 Gbps data rate

IV. CONCLUSION

In conclusion, a PN-type carrier-induced silicon waveguide Bragg grating formed by ion implantation technology was demonstrated. The extinction ratio of the grating filter is 19 dB. The extinction ratio modulation is realized under both reverse bias and forward bias. Under the reverse bias, an extinction ratio of more than 11.5 dB is achieved. Under the forward bias, an extinction ratio of more than 10 dB is achieved. The central wavelength shifting rates under forward and reverse biases are -1.25 nm/V and 0.01 nm/V, respectively. The modulation

frequency of this carrier-induced is very fast and the eye-diagram of 8 Gpbs data rate is achieved. With increase the reverse bias, the optical loss reduces. The reduction of optical loss is 1.5 dB under the reverse bias of -20 V. This kind of carrier-induced grating can be used as a special wavelength selective switch. Without any bias, it is used as a normal filter. With a reverse bias, it can guide all waves as a normal waveguide, keeping a low optical loss.

#### ACKNOWLEDGMENTS

The author would like to thank National Natural Science Foundation of China (Grant No. 61177064) and Singapore A\*STAR SERC Grant No.1122804038 for support.

#### REFERENCES

- [1] H. Tsuda, "Fiber Bragg grating vibration-sensing system, insensitive to Bragg wavelength and employing fiber ring laser," *Opt. Lett.* 35, pp. 2349-2351 (2010).
- [2] Y. G. Han and S. B. Lee, "Tunable dispersion compensator based on uniform fiber Bragg grating and its application to tunable pulse repetition-rate multiplication," *Opt. Express* 13, pp. 9224-9229 (2005).
- [3] D. T. H. Tan, et al., "Cladding-modulated Bragg grating in silicon waveguides," *Opt. Lett.* 34, pp. 1357-1359 (2006).
- [4] S. Honda, et al., "Largely-tunable wideband Bragg gratings fabricated on SOI rib waveguides employed by deep-RIE," *Electron. Lett.* 43, pp. 630-631 (2007).
- [5] G. Jiang, et al., "Slab-modulated sidewall Bragg grating in silicon-on-insulator ridge waveguides," *IEEE Photon. Technol.* 23, pp. 6-8 (2011).
- [6] Q. Fang, et al., "Carrier-induced silicon Bragg grating filters with a p-i-n junction," *IEEE Photon. Technol.* 25, pp. 810-812 (2013).